JOURNAL OF SOLID STATE CHEMISTRY 21, 57–65 (1977)

Phases and Phase Transitions of Compounds $(C_nH_{2n+1}NH_3)_2MnCl_4$ with $n = 1, 2, 3$

W. DEPMEIER,* J. FELSCHE, AND G. WILDERMUTH

Universität Konstanz, Lab. Festkörperchemie, Postfach 7733, D-7750 Konstanz, Germany

Received September 3, 1976; in revised form December 20, 1976

Phases and structural phase transitions of the compounds $(CH_3NH_3)_2MnCl_4$, $(C_2H_5NH_3)_2MnCl_4$ and $(C_3H_7NH_3)_2MnCl_4$ have been studied by means of thermoanalytical methods (DSC) and X-ray single crystal and powder diffraction data in the temperature range of 85–480°K at normal pressure. All phases show perovskite-like layer structures. The high temperature phases (α phase) correspond to the K_2NiF_4 type and may be regarded as the aristotype of each polymorphic compound. All transitions are reversible. Transition patterns are:

$$(CH_3NH_3)_2MnCl_4: \alpha \xleftrightarrow{398°K} \beta \xleftrightarrow{257°K} \gamma \xleftrightarrow{92°K} \delta$$

$$(C_2H_5NH_3)_2MnCl_4: \alpha \xleftrightarrow{424°K} \beta \xleftrightarrow{225°K} \gamma$$

$$(C_3H_7NH_3)_2MnCl_4: \alpha \xleftrightarrow{446°K} \beta \xleftrightarrow{396°K} \gamma \xleftrightarrow{344°K} \delta \xleftrightarrow{165°K} \varepsilon \xleftrightarrow{110°K} \zeta$$

Based on the DSC peak-shape analysis and diffraction data a model of a tilting system of the $MnCl_6$-octahedra layer is introduced in order to understand essential features of structures of different phases and their transition behavior. Single crystal film data of $(C_3H_7NH_3)_2MnCl_4$ phases reveal some disorder phenomena. The ε phase exhibits a superstructure along [010] with a triplication of the shortest axis corresponding to the δ phase. The γ phase of this compound shows strong satellite reflections, due to a transverse distortion wave along the [100] lattice direction.

Introduction

The group of compounds $(C_nH_{2n+1}NH_3)_2MCl_4$ with $M = Mn$, Cd is of increasing interest because of some unique properties (*1*) of these crystals. Existence of a number of phases and different types of phase transitions is one attraction from the view of structural chemistry (*2–11*). Up until now the methyl compounds have been studied in detail (*7–11*). We started our investigations on the ethyl and propyl compounds with $M = Mn$ in order to show the influence of the length of the alkyl chain on the structural phase characteristics as well as on the transition behavior. Methods employed were differential scanning calorimetry and X-ray and neutron diffraction in the temperature range of 85–480°K. Some of the results will be presented in this paper on $(CH_3NH_3)_2MnCl_4$, $(C_2H_5NH_3)_2MnCl_4$, and $(C_3H_7NH_3)_2MnCl_4$ which will subsequently be designated C1Mn, C2Mn, and C3Mn, respectively. Special data on crystal structures of individual phases taken at different temperatures and other results concerning the mechanisms of phase transitions and decomposition reactions will be published elsewhere. So far crystal structure data on the room temperature (β) phase of C2Mn has been published (*12*), and some details on the low-temperature (γ) phase and

* To whom correspondence should be addressed.

ISSN 0022-4596

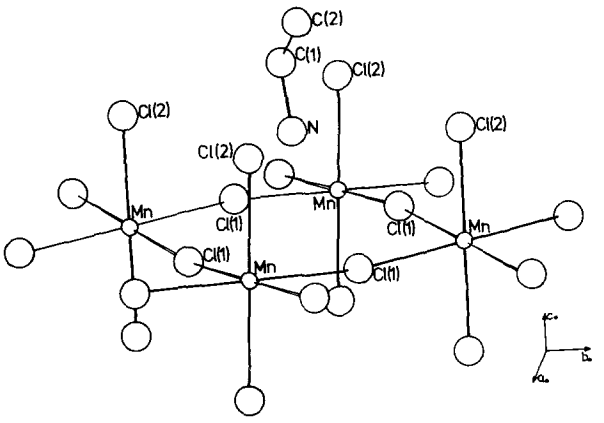

FIG. 1. Crystal structure of the β-phase of $(C_2H_5NH_3)_2MnCl_4$ (in part) showing the nitrogen position surrounded by eight chlorines. Hydrogen atoms are not shown.

the γ–β phase transition have been reported (*6*). Some results of differential scanning calorimetry on $(C_nH_{2n+1}NH_3)_2MnCl_4$ have also been published recently (*13*).

According to (*12*) and (*15*) a general feature of the C1Mn, C2Mn, and C3Mn crystal structures is shown to be a two-dimensional arrangement of corner-sharing $MnCl_6$ octahedra. With respect to the family of perovskite structures this layer represents a section of *B* sites occupied by Mn^{2+} ions.

As shown in Fig. 1 four of the six chlorine atoms (Cl(1)) surrounding the Mn^{2+} ion connect neighboring octahedra while the negative charge is concentrated on the remaining two chlorines (Cl(2)). The elongated alkyl-ammonium ions are arranged on positions nearly perpendicular to the $MnCl_6$-octahedra layer. This position corresponds to the *A* site of a perovskite structure. The orientation of the $(RNH_3)^+$ groups is such that the $-NH_3$ residue points toward the layer while the alkyl residue points away from it. Adjacent layers form van der Waals contacts. They show staggered orientation, the tip of each octahedron pointing to a void of the neighboring layer. All the chlorine atoms can act as acceptors for N–H . . . Cl hydrogen bonds. The position of the $-NH_3$ group is free to take various orientations with respect to the eight chlorine atoms.

Models of thermal stability of individual structures and phase transitions have been discussed (*7*, *10*, *12*), for C1Mn, C2Mn, and C1Cd. Forced by changes in the thermal motion of the alkyl-ammonium group, the switching of the $-NH_3$ group between different orientations is proposed to be responsible for all phase transitions so far known. Obviously a lengthening of the alkyl chain influences this motion so that different transition patterns are to be expected for C2Mn and C3Mn compounds. It will be shown here that in addition to the thermal motion of the alkyl-ammonium groups orientation changes inside the $MnCl_6$-octahedra layers may be responsible for the mechanism of phase transitions.

II. Experimental

Crystals were grown from aqueous solutions of CH_3NH_3Cl, $C_2H_5NH_3Cl$, or $C_3H_7NH_3Cl$, and $MnCl_2$. The strongly hygroscopic crystals show incongruent melting. On being heated in air the compounds even decompose at temperatures below the $\beta \rightarrow \alpha$-transition, i.e., before they reach their *aristotype* structure.[1] Therefore capillaries were used for single crystal X-ray work and crystal powders were embedded in Cellit L 700 in order to prevent sublimation of RNH_3Cl during the long term experiments.

[1] For a discussion of the term *aristotype* see: H. D. Megaw, Crystal Structures: A Working Approach, 1973, W. B. Saunders, Philadelphia/London/Toronto.

This procedure was successful for all three compounds C1Mn, C2Mn, and C3Mn up to 500°K.

Both X-ray and neutron diffraction techniques were used, the latter with a four-circle diffractometer at the reactor at Karlsruhe and at the I.L.L. (Grenoble). The X-ray techniques with Mo and Cu radiation involve single crystal diffractometry on a two-circle diffractometer as well as Weissenberg and precession film techniques supplemented by heating and cooling devices for temperatures of 85–1000°K. Furthermore, temperature-controlled Guinier techniques for both single crystals and powder specimens were used. A Guinier–Lenné camera served to determine the unit cell dimensions at low temperatures down to 130°K while a high-resolution Guinier–Huber chamber 631/632 was used at elevated temperatures of up to 500°K. Silicon was used as internal standard for the diffraction patterns from which the unit cell dimensions were determined by least-squares refinement (*14*).

The long-term stability of the PID-temperature control was ±2°K for the high and low temperature work with the single crystal and powder camera. However, the large temperature gradient in the heating zone of the Guinier-Huber chamber 631/632 showing a U-shaped geometry of the heating device increased the error of this temperature data to ±8°K. Therefore, the data of the temperature dependence of the unit cell parameters of C2Mn and C3Mn as shown in Figs. 6 and 7 were taken from different runs on the Guinier–Lenné camera as well as from the Guinier–Huber camera using powder samples. The interesting slope of the curves of C3Mn in Fig. 7 was confirmed by single crystal Guinier photographs. These photographs of special groups of reflections proved to be an excellent help in the interpretation of crossing lines on heating powder photographs, especially in the region of higher diffraction angles. Employing a double bent Johansson monochromator provides an extreme sensitivity of the diffraction pattern on the crystal's "individually," e.g., inclusions, coatings, and mounting.

For calorimetric measurements in the temperature range 87–500°K, a Perkin–Elmer DSC-2 differential scanning calorimeter was used with He atmosphere. For temperature calibration, the transition temperature of cyclohexane (186.1°K) and the melting point of indium (429.78°K) have been employed, the heat of transition of indium serving as well for the calorimetric calibration ($\Delta H = 6.80$ cal/g). Specimens used were dried single crystals of weight 30–50 mg enclosed in an aluminium pan. Heating rates employed were 10, 20, or 40°K/min, intensity scales were 1 or 5 mcal/sec.

For DSC-peak shape analysis, the intercept between the extrapolated reference lines and the tangent to the rising side of the peaks was chosen as the transition temperature for discontinuous transitions (C1Mn, 92 and 257°K; C3Mn, 110°K). For those peaks where the transition character is not confirmed to be discontinuous, we report the DSC-peak maximum as the transition temperature. Generally, transition temperatures have been determined from heating cycles.

To obtain the enthalpies of the transitions the peak areas have been measured by a disk integrator. Several measurements on different samples served to determine a mean value. Entropy changes have been simply calculated from $\Delta S = \Delta H/T$. In cases such as the 165°K transition of C3Mn where the reaction occurs over a wide range of temperature the relatively low values of enthalpy have been roughly estimated from the peak areas. There is no reliable procedure known for evaluating quantitatively such reaction characteristics in differential scanning calorimetry.

Results and Discussion

Data for the structural phase transitions as observed by differential scanning calorimetry and diffraction work will be presented in this paper without extensive discussion of the individual structures in terms of bond lengths and angles. Reliable data on the structures above and below the transition points, needed to discuss the mechanisms of transition, are still missing in most cases. So far little information is available in the literature for the various phases of C3Mn. The room temperature structure is known (*15*), but there remains some

TABLE I

CRYSTAL DATA AND TRANSITION CHARACTERISTICS FOR PHASES OF $(CH_3NH_3)_2MnCl_4$ (α, β, γ, δ), $(C_2H_5NH_3)_2MnCl_4$ (α, β, γ) AND $(C_3H_7NH_3)_2MnCl_4$ (α, β, γ, δ, ε, ζ)[a]

$(CH_3NH_3)_2MnCl_4$	$(C_2H_5NH_3)_2MnCl_4$	$(C_3H_7NH_3)_2MnCl_4$
α	α	α
SG: I4/*mmm*, $Z = 2$	SG: I4/*mmm*, $Z = 2$	SG: I4/*mmm*, $Z = 2$
$a =$ 5.133(4) Å $c =$ 19.51(1) Å at 404°K (*8*)	$a =$ 5.20(1) Å $b =$ 5.20(1) Å $c =$ 22.33(5) Å	$a =$ 5.20(1) Å $b =$ 5.20(1) Å $c =$ 27.89(5) Å
398°K (P) continuous	424°K (P) continuous	446°K (P) continuous
β	β	β
SG: *Abma*, $Z = 4$ $a =$ 7.276(3) Å $b =$ 7.215(3) Å $c =$ 19.41(1) Å at 293°K (*12*)	SG: *Abma*, $Z = 4$ $a =$ 7.353(1) Å $b =$ 7.258(1) Å $c =$ 22.087(4) Å at 295°K	SG: *Abma* (?), $Z = 4$ $a =$ 7.40(1) Å $b =$ 7.34(1) Å $c =$ 27.45(10) Å at 400°K
257°K (*T*) discontinuous $\Delta H = 27 \pm 0.5$ cal/mole $\Delta S = 0.11$ cal mole^{-1}K^{-1}	225°K (P) discontinuous (w.p.r.) $\Delta H = 156 \pm 3$ cal/mole $\Delta S = 0.7$ cal mole^{-1}K^{-1}	396°K (P) discontinuous (w.p.r.) $\Delta H = 60 \pm 5$ cal/mole $\Delta S = 0.15$ cal mole^{-1}K^{-1}
γ	γ	γ
SG: $P4_2/ncm$, $Z = 4$ $a =$ 7.23(1) Å $c =$ 19.32(2) Å at 188°K (*12*)	SG: *Pbca*, $Z = 4$ $a =$ 7.325(8) Å $b =$ 7.151(10) Å $c =$ 22.08(19) Å at 127°K	SG: *Abma* (?), $Z = 4$ $a =$ 7.42(1) Å $b =$ 7.30(1) Å $c =$ 26.97(5) Å at 365°K, "subcell data"
92°K (*T*) discontinuous $\Delta H = 164 \pm 4$ cal/mole $\Delta S = 180$ cal mole^{-1}K^{-1}		344°K (P) discontinuous (w.p.r.) $\Delta H = 190 \pm 5$ cal/mole $\Delta S = 0.56$ cal/mole°K^{-1}
δ		δ
SG: $P2_1/a$, $Z = 4$ $a =$ 7.13 Å $b =$ 7.25 Å $c =$ 19.30 Å $\beta = 92.17°$		SG: *Abma*, $Z = 4$ $a =$ 7.462(3) Å $b =$ 7.247(3) Å $c =$ 25.80(2) Å at 293°K
		$a =$ 7.458(9) Å $b =$ 7.169(9) Å $c =$ 25.61(5) Å at 182°K
		165°K (P) discontinuous (w.p.r.) $\Delta H = 12$ cal/mole
		ε
		SG: *Pbca*, $Z = 12$ $a =$ 7.45 Å $b =$ 21.41 Å $c =$ 25.54 Å at 130°K
		110°K (*T*) discontinuous $\Delta H = 101 \pm 2.5$ cal/mole $\Delta S = 1$ cal mole^{-1}K^{-1}
		ζ

[a] "Discontinuous w.p.r." means "discontinuous with preliminary region," "P" or "T" means transition temperature from peak maximum or tangent/reference line interception, respectively. For further explanation see text. SG = space group.

question about the real orientation of the alkyl-ammonium group and the hydrogen-bonding scheme. For structural data on C1Mn and C1Cd see Refs (*7–11*); results for C2Mn will be published shortly (*16*, *17*).

For consistency in designating the different thermodynamically stable phases of compounds C1Mn, C2Mn, and C3Mn we decided to use Greek letters throughout this paper. A summary of the calorimetric data combined with unit cell dimensions is shown in Table 1. Terms "continuous" or "discontinuous" are used to describe the character of the phase transition. "Continuous" phase transitions definitely show supergroup/subgroup relations in the space group symmetry of the corresponding crystal structures. The term "discontinuous with preliminary region" (henceforth designated discontinuous w.p.r.) was used for transitions which are characterized by an increase of heat capacity over a wide range of temperature close to the transition point (compare the transitions of C3Mn at 110 and 344°K in Fig. 4 as examples for discontinuous and discontinuous w.p.r. transitions). We feel that all these transitions are of the same kind. From our knowledge of the γ–β transition of C2Mn (see below) we assume that they are connected with orientation switching. Figures 2–4 show the original heat flux (dq/dt) vs temperature curves from the DSC-2 recorder for compounds C1Mn, C2Mn, and C3Mn close to the transition points. (Measuring dq/dt corresponds to the determination of the change of enthalpy, which in turn corresponds to the heat capacity). Structural data on some phases are introduced in Figs. 5–7 in order to explain the phase transitions. Figure 5 gives a schematic representation of the different structures of C1Mn. Figures 6 and 7 show plots of unit cell dimensions vs temperature for C2Mn and C3Mn. Phase sequences have recently been studied for C1Mn and C1Cd (*7–11*). From these investigations some structural characteristics of different phases are known which are also relevant for C2Mn and C3Mn. The essential feature of all the structures has been described in terms of the RNH_3-group orientation (or hydrogen bonding schemes) (*7–11*). The various possible $-NH_3$-group

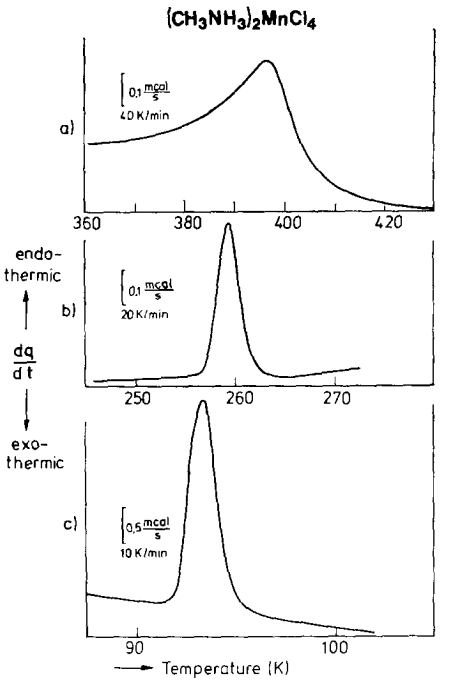

FIG. 2. Differential scanning calorimetric curves of $(CH_3NH_3)_2MnCl_4$ showing (a) the $\beta \rightarrow \alpha$, (b) the $\gamma \rightarrow \beta$, and (c) the $\delta \rightarrow \gamma$ phase transition.

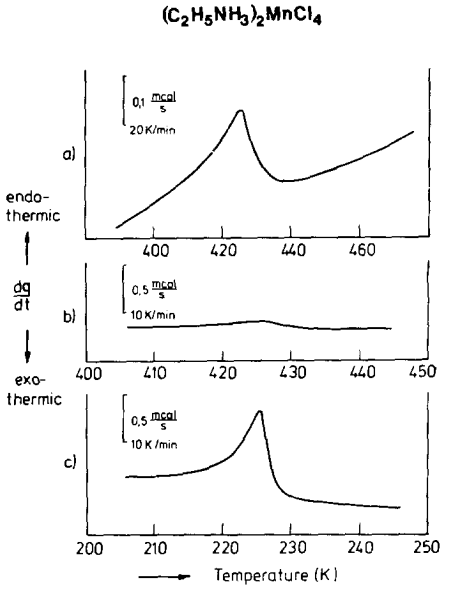

FIG. 3. Differential scanning calorimetric curves of $(C_2H_5NH_3)_2MnCl_4$. Both (a) and (b) show the $\beta \rightarrow \alpha$ transition, but with different heating rates and intensity scales. The (c) curve is from transition $\gamma \rightarrow \beta$.

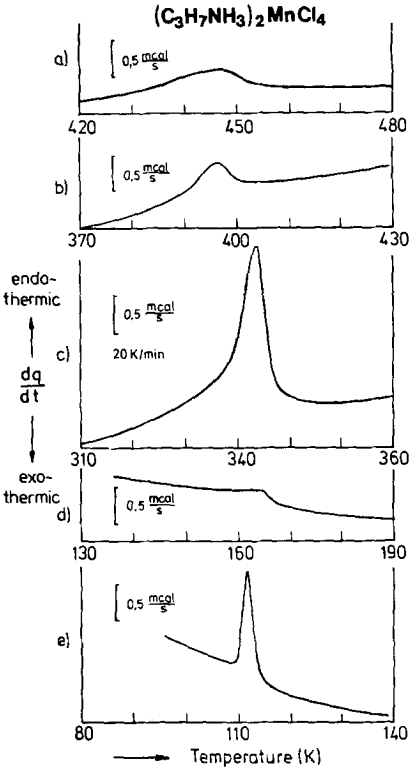

FIG. 4. Differential scanning calorimetric curves of $(C_3H_7NH_3)_2MnCl_4$ showing (a) the $\beta \rightarrow \alpha$, (b) the $\gamma \rightarrow \beta$, (c) the $\delta \rightarrow \gamma$, (d) the $\varepsilon \rightarrow \delta$, (e) the $\zeta \rightarrow \varepsilon$ phase transition. All runs with heating rate 20°K/min.

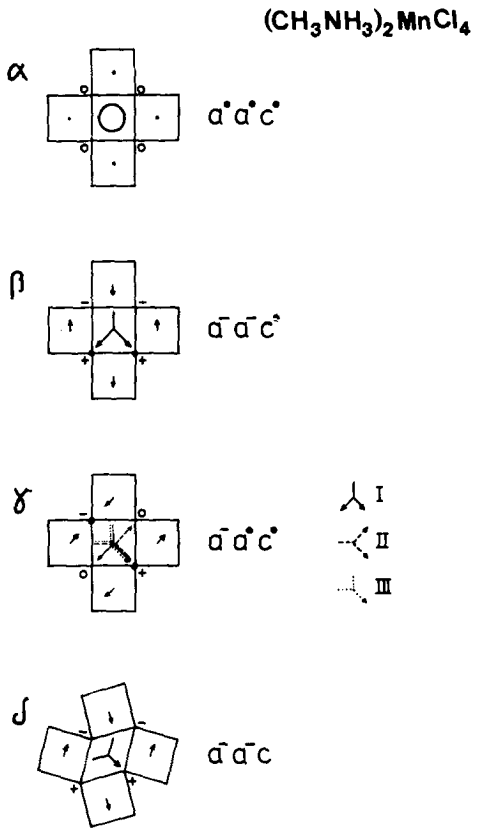

FIG. 5. Schematic representation of tilting systems and NH_3-group orientations for $(CH_3NH_3)_2MnCl_4$ phases. Projections along [001] show the characteristics for the α-, β-, γ- and δ-phase crystal structures. Squares represent the corner-sharing $MnCl_4$-units, which surround the nitrogen. The circle symbol of the α phase means complete rotational disorder for the NH_3 group. Bars and arrows in the β-, γ- and δ-phase indicate hydrogen bonds directed to axial Cl(2) or equatorial Cl(1), respectively, which correspond to the Cl positions in Fig. 1. The tilts of the squares formed by Cl(1) are represented by arrows (or points in the α phase) which furthermore show the displacement of the Cl(2) from the position in the *aristotype*. Displacements of Cl(1) from the plane of the manganese are designated by ○, − or +. Note the superposition of hydrogen bonding systems I, II, III in the tetragonal γ phase. For explanation of designations such as $a^0a^0a^0$, see text.

orientations may be divided into two classes. First, two hydrogen bonds may run to corner-sharing Cl(1) atoms, while one hydrogen bond points to an axial Cl(2) atom. Secondly, two hydrogen bonds may run to two axial Cl(2) atoms while another points to an equatorial Cl(1). We follow (*8*) and call the former bonding scheme orthorhombic and the latter monoclinic.

We feel, however, that another essential feature of the structures should be discussed in order to show the differences between individual phases, namely the orientation shifts within the $MnCl_6$-octahedra layer. In Fig. 5 this approach is demonstrated for ClMn structures in terms of a tilt system of corner-sharing octahedra. The symbols used correspond closely to the notation for tilted octahedra in perovskite structures as given by Glazer (*18*). In Glazer's paper the notation $a^-b^-c^+$ means tilts about the directions [100], [010], and [001], respectively, the directions referring to the cubic axes of the *aristotype* structure. If tilts about different directions

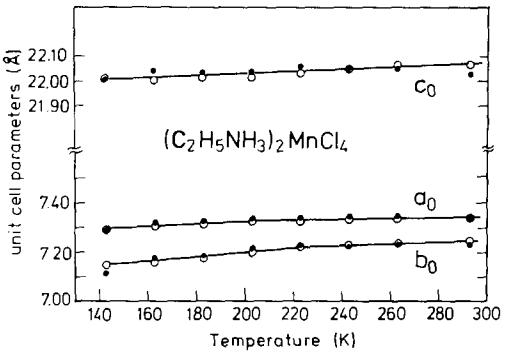

FIG. 6. Unit cell parameters vs temperature around the $\gamma \rightarrow \beta$ transition for $(C_2H_5NH_3)_2MnCl_4$. Full and open circles denote results from different samples.

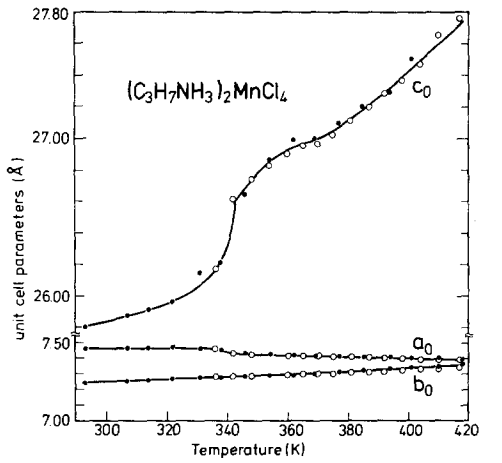

FIG. 7. Unit cell parameters vs temperature around the $\delta \rightarrow \gamma$ and $\gamma \rightarrow \beta$ transitions for $(C_3H_7NH_3)_2MnCl_4$. Full and open circles denote results from different samples.

have equal amplitude, then the same letter is used, e.g., $a^-a^-c^+$. The superscript + means that along a tilt axis octahedra are tilted *in phase*, whereas the superscript − means that octahedra are tilted *in antiphase*.

Glazer's original notation has been applied to a three-dimensional corner-sharing octahedra system. In the case of the K_2NiF_4-structure type which may be looked at as the *aristotype* for C1Mn, C2Mn, and C3Mn, the notation refers to a two-dimensional system of corner-sharing squares (more correctly: to corner-sharing rectangles). Thus the notation is similar to that for the perovskite structures, the difference being that the third symbol needs no superscript to distinguish between *in phase* and *in antiphase*.

The α phase of C1Mn is characterized by an $a^0a^0c^0$-tilt system, which means that in their average positions the Mn^{2+} ions and chlorines Cl(1) are in plane. In this case the NH_3-bonding system represents a completely disordered orthorhombic configuration. The $\beta \rightarrow \alpha$ transition is continuous over a wide range of temperatures (380–420°K). The β phase, which is the stable room temperature form, exhibits an $a^-a^-c^0$ tilt system and an orthorhombic NH_3 configuration.

The transition to the next phase, the tetragonal γ phase, is a discontinuous one with relatively low values for ΔH and ΔS. This transition is one of the rare examples in the field of structural phase transitions where the low temperature form shows a higher symmetry than the high temperature form. The tilt system of the γ phase is now $a^-a^0c^0$, i.e., there is only one tilt left. The NH_3–hydrogen bonding scheme is a superposition of two orthorhombic and one monoclinic configuration.

Another discontinuous transition leads to the monoclinic δ phase. This transition is marked by a ΔH of 164 cal $mole^{-1}$ and an entropy change of 1.80 cal $mole^{-1}$ $°K^{-1}$, thus indicating that the structures on both sides are not as closely related as were the β and γ phases. In fact, there are again two tilts of equal amplitude but, in addition, there is a tilt in the [001] direction, thus giving an a^-a^-c system. The geometry of the cavities allows only one single monoclinic NH_3 configuration.

The schematic tilt system representation of Fig. 5 is largely based on structural data of analogous C1Cd structures, which have the most accurate data from X-ray structure analysis (*8*, *10*). For a complete representation of the hydrogen-bonding scheme on C1Cd see (*8*, Table V). It seems worthwhile mentioning that the α phases of C1Mn and C1Cd show some significant differences with respect to the N and C positions (*8*, *10*). The dependence of lattice parameters on temperature for C1Mn is almost linear. Contrary to the compounds C2Mn and C3Mn there are no un-

usual features in the temperature ranges of transition points.

The phase sequence of C2Mn is simpler than that of C1Mn. The α phase again has the K_2NiF_4 structure, i.e., tilt system $a^0a^0c^0$, and probably disordered or rotating $C_2H_5NH_3$ groups. A continuous transition leads to the orthorhombic β phase which has the same $a^-a^-c^0$ tilt system as the methyl derivative but different NH_3 orientation. Neutron diffraction results have shown that there are two superimposed monoclinic configurations (related by the mirror plane of space group *Abma*) and possibly one orthorhombic configuration (*16*). The latter, however, is included in the superposition of the two former configurations.

The transition to the γ phase has a ΔH of the same order of magnitude as the 92°K transition of C1Mn. Actually, by X-ray diffraction it has been shown that the γ phase also exhibits the a^-a^-c tilt system. Furthermore, the NH_3 configuration is simply monoclinic (*17*). However, one interesting property should be emphasized. The peak in the heat capacity vs temperature curve is smeared out over a considerable temperature range. Moreover, there is a shift in the heat capacity (see Fig. 3c). We interpreted this behavior as an orientation switching where the $C_2H_5NH_3$ groups are increasingly disordered during a heating run within a preliminary region up to the point where ordered and disordered orientations are no longer distinguishable, i.e., where the transition occurs. This kind of transition seems to be characteristic of longer-chained members of this class of compounds. This phenomenon may best be demonstrated by comparing C3Mn with C1Mn.

Figure 6 shows the change of the unit cell dimensions between 140°K and room temperature. The temperature dependence is almost linear for both phases, the 225°K transition being indicated by a significant change in the slope of curves for the a_0 and b_0 axes.

The transition pattern of C3Mn is more complex than that of C1Mn or C2Mn. So far only the δ phase (room temperature form) is known from X-ray structure analysis (*15*). The NH_3-group orientation, however, seems doubtful in this study which was done at room temperature. Therefore, we did some additional neutron diffraction work at 180°K in order to provide more information about the hydrogen positions, i.e., the hydrogen bonding scheme (*19*).

From the DSC data (Fig. 4) it can be seen that the $\beta \rightarrow \alpha$ transition of C3Mn is a continuous one. We assume that the high-temperature form (α phase) has the tetragonal K_2NiF_4 structure with disordered $C_3H_7NH_3$ groups and an $a^0a^0c^0$ tilt system. On the other hand, we expect an a^-a^-c tilt system for the ζ-phase structure from the $\zeta \rightarrow \varepsilon$ transition characteristics. This must be verified, however, by diffraction studies below 110°K. All three remaining transitions $\beta \rightarrow \gamma$, $\gamma \rightarrow \delta$, $\delta \rightarrow \varepsilon$ are of the kind we call discontinuous w.p.r. Little information is available about the structures of phases β, γ, ε, and ζ. However, on single crystal X-ray photographs some of these phases reveal interesting features.

The ε phase is characterized by a triplication of the b axis with respect to the δ phase. We plan to study this superstructure by neutron diffraction in the near future. Other than triplication of the b axis there is no remarkable change in the unit cell dimensions. The symmetry of the structure is lowered to give space group *Pbca*.

The 344°K transition is most prominent in Fig. 4 and also in Fig. 7 where lattice dimensions are plotted against temperature. The $\delta \rightarrow \gamma$ transition is marked by a very strong dependence of c_0 on the temperature. A preliminary region with rapidly increasing c_0 is followed by the transition itself with a shift of nearly 0.4 Å. With increasing temperature there is a further increase of the c_0 value but with reversed curvature. After the turning point the slope becomes almost linear. Parallel to this surprising variation in c_0 there is a remarkable decrease of a_0 at the transition, whereas b_0 does not seem to be influenced by this transition. The formation of the γ phase is accompanied by the appearance of strong, sharp satellite reflections which are arranged around the extinct main reflections with $k + l = 2n + 1$.

The satellites are located on rods parallel to

a^*. The a_0 dimension of the superstructure is 42.3 Å. The ratio of a_0 (super cell):a_0 (sub-cell) is 5.7. No satellites appear in the $hk0$ layer. These features are compatible with a transverse distortion wave running in the direction of the a axis with its amplitude parallel to the c axis (*20*). Atoms related by the A centering are influenced by two distortion waves which have a phase shift of π relative to each other. From the following facts we conclude that the Cl(2) atoms in connection with hydrogen bonds are mainly influenced by the distortion waves.

These facts are:

(a) The satellites are relatively strong, indicating that atoms which are involved have relatively strong scattering power.

(b) The amplitude of the distortion wave is parallel to the c axis.

(c) The c_0 lattice constant is markedly increased.

It is not yet known in detail what happens at this transition. Therefore, we plan to do X-ray and neutron diffraction work on this phase in the near future.

The 396°K β–γ transition is revealed only by DSC measurements. No significant changes of lattice dimensions occur at the transition. At present we know nothing about the structure of the β phase. It seems to change continuously into the tetragonal *aristotype* of the α phase.

It seems worthwhile mentioning that the analogous cadmium compound C3Cd exhibits a transition pattern which is totally different from that of C3Mn (*5*).

Acknowledgments

We wish to acknowledge the helpful discussion with our colleagues at the ETH Zurich/Lausanne, University of Zurich and Dr. H. Arend's advice in preparing the crystals.

We thank Mrs. E. Neumann and Mrs. A. Skorczyk-Schrader for their help with drawings.

References

1. L. H. de Jongh and A. R. Miedema, *Adv. Phys.* **23**, 1 (1974).
2. H. Arend, R. Hofmann, and F. Waldner, *Solid State Commun.* **13**, 1629 (1973).
3. H. Arend, R. Hofmann, and J. Felsche, *Ferroelectrics* **8**, 413 (1974).
4. R. Kind and J. Roos, *Phys. Rev. B* **13**, 45 (1976).
5. G. Chapuis, presented at the Informal Meeting on Halide Perovskite Layer Structures, Zürich, 1976.
6. W. Depmeier, presented at the Informal meeting on Halide Perovskite Layer Structures, Zürich, 1976.
7. G. Chapuis, H. Arend, and R. Kind, *Phys. Status Solidi* **31**, 449 (1975).
8. G. Chapuis, R. Kind, and H. Arend, submitted for publication.
9. J. Seliger, R. Blinc, R. Kind, and H. Arend, submitted for publication.
10. G. Heger, D. Mullen, and K. Knorr, *Phys. Status Solidi (a)* **31**, 455 (1975).
11. G. Heger, D. Mullen, and K. Knorr, *Phys. Status Solidi (a)* **35**, 627 (1976).
12. W. Depmeier, *Acta Crystallogr.* **B32**, 303 (1976).
13. E. H. Bocanegra, M. J. Tello, M. A. Arriandiaga, and H. Arend, *Solid State Commun.* **17**, 1221 (1975).
14. D. Schwarzenbach, "Latcon. A General Program for the LS-Refinement of Lattice Constants", ETH, Zürich (1971).
15. E. R. Peterson and R. D. Willett, *J. Chem. Phys.* **56**, 1879 (1972).
16. W. Depmeier and G. Heger, to appear.
17. W. Depmeier, to appear.
18. A. M. Glazer, *Acta Crystallogr.* **B28**, 3384 (1972).
19. W. Depmeier and S. A. Mason, to appear.
20. H. Schulz, *Acta Crystallogr.* **B30**, 1318 (1974).